Radiocarbon (2025), **67**, pp. 600–612
doi:10.1017/RDC.2025.19

CAMBRIDGE UNIVERSITY PRESS

RESEARCH ARTICLE

Reservoir Effects from Shells of Tell Abraq, Sharjah Emirate, UAE

Susanne Lindauer[1], Marc Händel[2] and Peter Magee[3]

[1]Curt-Engelhorn-Centre Archaeometry gGmbH, C4, 8, 68159 Mannheim, Germany, [2]Austrian Archaeological Institute, Austrian Academy of Sciences, Vienna, Austria and [3]Zayed National Museum, Department of Culture and Tourism, Abu Dhabi, UAE
Corresponding author: Susanne Lindauer; Email: susanne.lindauer@ceza.de

Received: 11 January 2023; **Revised:** 21 January 2025; **Accepted:** 26 January 2025; **First published online:** 19 May 2025

Keywords: Arabia; archaeology; radiocarbon; reservoir effect; shells

Abstract
We present reservoir effects on shells of species *Terebralia palustris* and *Marcia spp.* that were recovered during archaeological excavations at the multi-period site of Tell Abraq, Sharjah Emirate, UAE (This paper was presented at the combined 24th Radiocarbon and 10th Radiocarbon & Archaeology International Conference, Zurich, Switzerland, Sept. 2022.). The site was inhabited during the mid to late Holocene. It is situated in a lagoonal environment with former mangrove forests at the Arabian Gulf coast of southeast Arabia. Due to availability in the immediate proximity, shellfish played an important role for the local subsistence throughout the site's occupation. Tell Abraq provides a well-defined and stratigraphically controlled archaeological context for investigations on the reservoir effect of the two species chosen. Crucial for the determination of the marine reservoir effect is comparison with contemporaneous terrestrial carbon samples. We discuss the data in a wider context with respect to results obtained at other sites.

Introduction

The Arabian Gulf coast in the northern United Arab Emirates (UAE) is characterized by numerous lagoons formed during the Holocene marine transgression in an interplay between oscillating sea level and influx of freshwater (and sediment) from fluvial activity or coastal aquifers (Bernier et al. 1995; Dalongeville and Sanlaville 2005; Lambeck 1996; Parker et al. 2018). In the past, lagoonal shores were often densely vegetated by mangroves forming highly productive habitats that played a significant role for mankind in the prevailing arid environment (Tengberg 2005). However, they are subject to evolutionary processes caused by changing environmental conditions. Today this is reflected by countless shell middens and extensive areas covered by shells from local subsistence scattered along the coast (Händel 2009, 2014).

The archaeological site of Tell Abraq is located at the end of the Umm al-Quwain lagoon of the northern UAE and is today divided between the Emirates of Sharjah and Umm al-Quwain. Tell Abraq is marked by a prominent mound and represents a landmark in the coastal landscape of shallow dunes and shell middens. The mound and its surroundings are characterized by architectural remains and large amounts of archaeological and zooarchaeological materials reflecting a long settlement history that lasted from ca. 2500 BCE to 300 CE (Potts 1991, 1993, 2000; Potts et al. 1990). Tell Abraq has seen several research episodes, starting in the 1970s. Systematic excavations between 1989 and 1998 established the cultural-chronological frame of the site's occupation and showed that the nucleus and earliest phase of the settlement was an early Bronze Age (Umm an-Nar-period) tower respectively elevated platform (Potts 1991; Potts et al. 1990). An Umm an-Nar tomb next to the tower provided substantial data regarding human demographics and health. Grave goods include objects imported from areas surrounding the Arabian Gulf, but also Mesopotamia, Baluchistan, the Indus valley, and Central

Asia (Blau 1996; Gregoricka 2014; Osterholz et al. 2014; Potts 1993). The full extent and spatial layout of the settlement was understood during the 2007–2017 excavations conducted in the Sharjah part of the site including the mound's surroundings (Magee et al. 2009, 2017, 2018). In 2019, excavations resumed in the Umm al-Quwain part of the site (Degli Eposti et al. 2022).

The 2nd millennium BCE saw a continuous expansion of the settlement's size including a stepped system of four terraces whereby the initial ∼8 m high tower formed the core of the uppermost terrace 1 (Magee et al. 2017, 2018). The retaining walls of terraces 3 and 4 were accompanied by ditches. Towards the exterior, the final construction displayed a massive roughly 4 m wide stone and mudbrick wall preserved ∼3 m high with a surrounding ∼3 m deep ditch. The (on-mound) terraces show sequences of plaster floors, bracketing occupation debris and providing well-stratified artifact and sample assemblages. Off-mound, the boundaries between occupation episodes are less sharp, but dug-out features such as hearths, pits and wells provide constrained sediment archives.

For this study, we collected shell and charcoal pairs from well-defined on- and off-mound contexts. This enabled investigating shells with respect to possible species-specific marine reservoir effects including temporal variation.

Marine shells usually result in ages older than their calendar age. The reason is uptake of radiocarbon depleted CO_2 from marine environments. The deep sea can store carbon for over 1000 years during which ^{14}C can decay (Lindauer 2019). In regions where this ^{14}C-depleted water is upwelling, such as the coast of Oman, it mixes with the surface water and is taken up by the organisms. Hence, the data needs to be corrected by considering a local marine reservoir effect ΔR, that is calculated as the difference between the marine radiocarbon age of the shell and the marine calibration curve that tries to account for a mean shift of the ocean waters. In addition, ΔR is species-specific, temporally variable due to changes in marine conditions such as upwelling, sea-level, freshwater input and depending on diet or habitat of the respective shell species (Culleton et al. 2006; Hadden and Cherkinsky 2016; Lindauer et al. 2017, 2022). In areas with reduced upwelling, the reservoir age can be less than the marine global mean and the corresponding ΔR might show negative values, otherwise the values are positive.

Paired measurements of shells and terrestrial material such as charcoal are ideal to monitor these changes over time. This information can also be used to improve the chronology of archaeological sites. Monitoring the species-specific reservoir effects for adjacent locations over time can help to reconstruct changes in environmental conditions not only on a local scale, but in comparison with other sites and proxies even on a global scale.

Material and methods

Charcoal and shell samples were recovered from archaeological contexts. On-mound, the samples derive from deposits bracketed by plaster floors. Off-mound, well-defined features such as hearths, pits and wells were chosen.

Sample locations are described by set and locus, whereby set refers to the anthropogenic feature, while locus specifies the locality within the excavation trench or set (Figure 1). All on-mound samples derive from trench 2. Loci 7722 and 7805 represent fills between plaster floors on terrace 2 consisting of compacted sand and archaeological materials (occupation debris). Ceramic typology and fabric of both fills attribute to the Middle Bronze Age (Wadi Suq). Locus 6252 is the fill of a hearth, located on terrace 3 and connected to Set 15 (Early to Middle Bronze Age ceramics), a group of hearths and ovens, stratigraphically situated beneath the sequence of plaster floors. It predates the creation of terrace 3 (Magee et al. 2017, Table 1). The stratigraphic sequence of the sampled on-mound loci is thus: 7722–7805–6252 (from younger to older).

The off-mound samples derive from trenches 205 and 207 with few architectural remains. Structures such as hearths, pits, and a deep well cut into the underlying archaeologically sterile sand provide suitable sampling locations predating Iron Age II (Magee et al. 2017). Locus 7230 is the fill of a pit

https://doi.org/10.1017/RDC.2025.19 Published online by Cambridge University Press

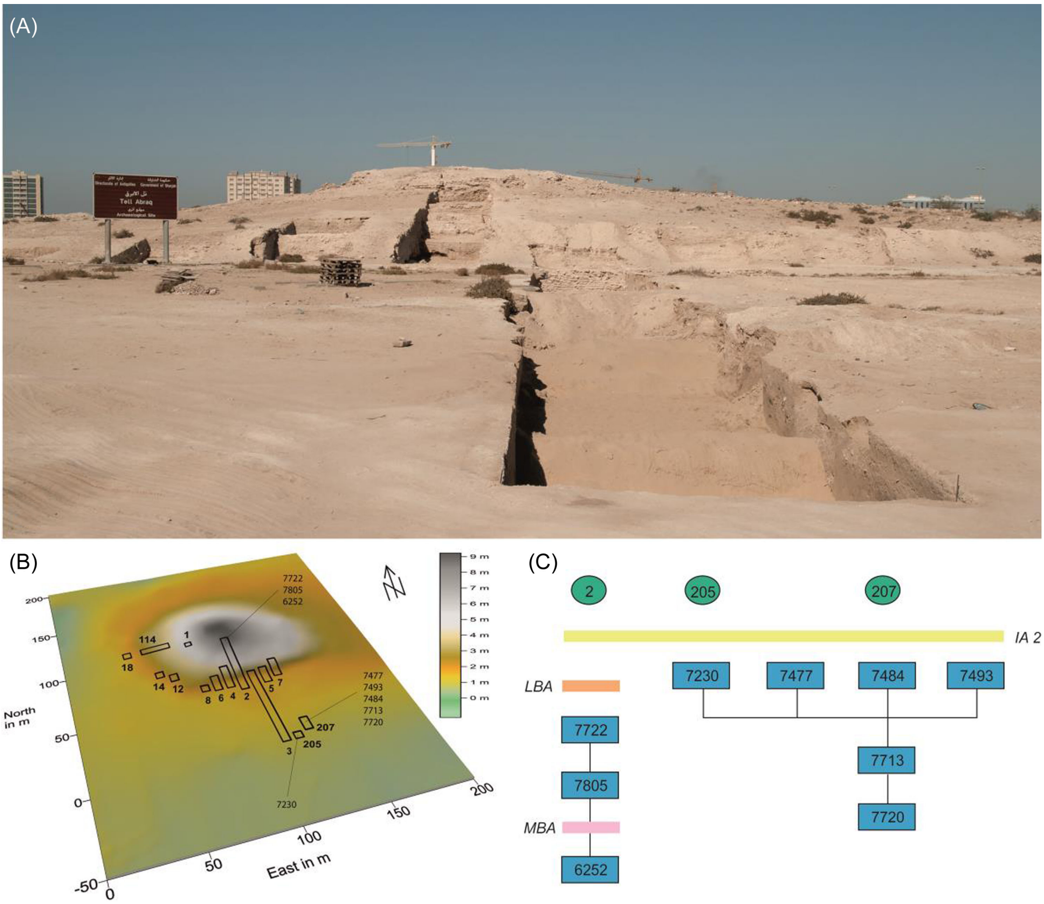

Figure 1. *(A) Photo of Tell Abraq mound, view to the north along trenches 3 and 2; (B) terrain model with excavation trenches (one to three digit numbers) and loci (four digit numbers); (C) stratigraphic matrix of archaeological contexts (loci) discussed with stratigraphic boundaries of main techno-cultural units (Photo and graphs: Marc Händel).*

(Set 67, trench 205) where morphology suggests rapid excavation and backfill. The loose fill showed a high density of shells. Ceramics indicate attribution to Late Bronze Age/Iron Age I. Locus 7477 (trench 207, Set 73) is the fill of a pit in comparable stratigraphic position and with similar size, morphology, and composition, but ceramics pinpointed to Iron Age I.

Locus 7493 (Set 73) is a pit mainly filled with shells, in this case *Terebralia sp.* fragments, but few other finds in a matrix of loose yellowish sand. The ceramic spectrum is classified as Late Bronze Age/ Iron Age I.

Locus 7484 (Set 73) is the fill of a pit with >2 m diameter. The occurrence of red Barbar ware suggests Early to Middle Bronze Age, a fabric indicating import from Dilmun. The well is cut into the underlying petrified palaeodune sequence; excavation reached a depth of ~4 m and didn't reach its base. We sampled its upper (Locus 7713) and lower (Locus 7720) fills. Both suggest rapid backfill.

The shells investigated are the gastropod *Terebralia palustris* and the bivalve *Marcia spp*. For *Terebralia palustris* it was already demonstrated that it shows a mixture of marine and terrestrial radiocarbon, as it feeds on mangrove leaves which display an atmospheric radiocarbon content due to photosynthesis (Lindauer et al. 2016). In contrast, *Marcia spp.* (often *flammea*) is a so-called filter feeder, i.e. its diet is influenced by the marine environment only. In addition, dissolved inorganic carbon

Table 1. *Radiocarbon dataset and results of reservoir effect modeling in Oxcal 4.4. using the IntCal20 and Marine20 datasets*

Lab code	Sample ID	Locus	Material	^{14}C age (yrs BP)	cal BCE (2σ)	ΔR (mean, yrs) 2σ
MAMS 30528	*18243-1 date seed*	7230	*Charcoal*	*2872 ± 20*	*1122–938*	
MAMS 30530	18243-2 Terebralia 2		Shell marine	3352 ± 20	1208–817	118 ± 48
P 15256	18243- Terebralia 4		Shell marine	3521 ± 21	1290–977	
P 15257	18243- Terebralia 5		Shell marine	3145 ± 20	1115–725	
MAMS 30980	18243-2 Terebralia 3		Shell marine	3425 ± 26	1261–891	
MAMS 30531	18243-3 Marcia 1		Shell marine	3455 ± 21	1187–974	109 ± 48
MAMS 30532	18243-3 Marcia 2		Shell marine	3438 ± 21	1183–970	
P 15258	18342- Marcia 3		Shell marine	3349 ± 24	1156–943	
P 15259	18342- Marcia 4		Shell marine	3405 ± 22	1173–960	
MAMS 30533	*18597-2 charcoal*	7477	*Charcoal*	*2883 ± 21*	*1190–986*	
MAMS 30534	18597-4 Terebralia 1		Shell marine	3361 ± 21	1216–822	1 ± 49
MAMS 30535	18597-4 Terebralia 2		Shell marine	3305 ± 22	1177–784	
P 15260	18597- Terebralia 3		Shell marine	3498 ± 22	1287–961	
P 15261	18597- Terebralia 4		Shell marine	3510 ± 29	1286–959	
MAMS 30536	18597-5 Marcia 1		Shell marine	3377 ± 22	1164–951	–23 ± 54
MAMS 30537	18597-5 Marcia 2		Shell marine	3398 ± 22	1172–958	
P 15262	18597- Marcia 3		Shell marine	3354 ± 23	1157–946	
P 15263	18597- Marcia 4		Shell marine	3334 ± 21	1151–940	
MAMS 32805	*18618 - charcoal*	7493	*Charcoal*	*3063 ± 23*	*1410–1261*	
P 15264	18618- Terebralia 1		Shell marine	3337 ± 22	1381–1187	–288 ± 64
P 15265	18618- Terebralia 2		Shell marine	3281 ± 21	1378–1174	
P 15266	18618- Terebralia 3		Shell marine	3203 ± 22	1381–1227	
P 15267	18618-Hexaplex 1		Shell marine	3428 ± 21	1480–1187	–112 ± 63
P 15268	18618- Hexaplex 2		Shell marine	3482 ± 22	1499–1210	
P 15269	18618- Hexaplex 3		Shell marine	3457 ± 20	1488–1200	
MAMS 46115	*18605–1 charcoal*	7484	*Charcoal*	*3074 ± 20*	*1411–1272*	
MAMS 46116	18605-2 Terebralia 1		Shell marine	4166 ± 22	1530–1305	Not used
MAMS 46117	18605-2 Terebralia 2		Shell marine	3927 ± 22	1526–1304	
MAMS 35984	*19309 charcoal*	7722	*Charcoal*	*3409 ± 21*	*1862–1624*	

(*Continued*)

Table 1. (*Continued*)

Lab code	Sample ID	Locus	Material	**^{14}C age** (yrs BP)	cal BCE (2σ)	ΔR (mean, yrs) 2σ
P 17778	19310 Terebralia		Shell marine	3879 ± 16	1808–1552	49 ± 78
P 17779	19311 Hexaplex		Shell marine	4109 ± 16	1970–1611	279 ± 76
MAMS 35983	*19421 charcoal*	7805	*Charcoal*	*3440 ± 23*	*1877–1641*	
MAMS 35989	19422 Terebralia		Shell marine	3913 ± 19	1811–1571	–27 ± 75
MAMS 35990	19443 Hexaplex		Shell marine	3881 ± 18	1865–1446	–61 ± 76
MAMS 46121	*19218 charcoal*	7713	*Charcoal*	*3492 ± 21*	*1885–1746*	
MAMS 46122	19219 Terebralia		Shell marine	3987 ± 28	1909–1733	Not used
	19219 Terebralia (dupl)		Shell marine	4187 ± 25	1947–1752	
MAMS 35982	*19259 charcoal*	7720	*Charcoal*	*3645 ± 22*	*2132–1941*	
MAMS 35987	19260 Terebralia		Shell marine	3812 ± 24	2062–1893	–262 ± 71
P 17777	19261 Hexaplex		Shell marine	4152 ± 13	2214–1861	46 ± 81
MAMS 35981	*14593 charcoal*	6252	Charcoal	*3668 ± 22*	*2137–1961*	
MAMS 35985	14593 Terebralia		Shell marine	4226 ± 21	2139–1987	85 ± 51
P 17780	14593 Terebralia		Shell marine	4222 ± 16	2139–1988	
MAMS 35986	14593 Marcia		Shell marine	4382 ± 23	2615–1894	298 ± 140
MAMS 46123	*19242 charcoal*	7720	*Charcoal*	*3728 ± 26*	*2202–2035*	
MAMS 46124	19243 Terebralia		Shell marine	4037 ± 27	2271–2041	–226 ± 61
	19243 Terebralia (dupl)		Shell marine	3919 ± 24	2245–2039	

in the sea water contributes to the shell. If available, both species were used for the same archaeological context to allow for a better species-specific monitoring of temporal changes. Another species that can be found throughout the Gulf of Oman and the Arabian Gulf is *Hexaplex kuesterianus.* This species is a predator and feeds on other mollusks, therefore, ΔR strongly depends on the preferred prey species. In this study, *H. kuesterianus* is included in the sampling strategy, despite this shortcoming. Results may support trends of the other species depending on preferred species for diet.

The samples were prepared in the radiocarbon laboratory of CEZA, Mannheim, Germany (labcode MAMS) and at the Max-Planck-Institute for Biogeochemistry in Jena, Germany (labcode P) using the identical preparation steps. Shells were sampled at the ventral margin, resulting in a mean radiocarbon age of the last few years of the mollusk´s life. Shell samples were pretreated using 1% HCl for about 1–2 minutes at room temperature to remove contamination resulting in a mass loss of around 30%. Charcoal samples were pretreated using ABA (for details see Lindauer et al. 2017). After pretreatment, the charcoal samples were combusted and catalytically converted to elemental carbon ("graphitization") using iron as catalyst before being pressed into a target and measured in a MICADAS type AMS system (Kromer et al. 2013; Lindauer 2019). For shell samples the carbon was extracted as CO_2 gas by adding phosphoric acid before graphitization (Lindauer 2019; Lindauer et al. 2017). Calendar ages and reservoir effects are modeled in Oxcal 4.4 using the IntCal20 and Marine20 datasets (Heaton et al. 2020; Ramsey 1995; Reimer et al. 2020) as described in (Lindauer et al. 2017; Zazzo et al. 2016).

Results and discussion

The uncalibrated, calibrated data and ΔR are presented in Table 1. ΔR for each species was modeled separately in Oxcal 4.4 using a phase model to help with the stratigraphical order of the loci (see Figure 2). During the modeling process we adjusted the prior probability U() of the respective phases until the model represented the best fit. The models for each species can be found in the supplement together with the representations of ΔR and the multiplots.

Not all data was used for modeling ΔR. The repeat measurement of shell MAMS 46122 of locus 7713 did not reproduce well without reason. Hence, it was decided to present it but not include it in the model. Locus 7484 was excluded as Oxcal always found it to be an outlier. From the archaeology it seems that this pit does not contain pairs that are strictly contemporaneous. However, all data is presented for completeness and in case a solution can be found in the future.

Interestingly, in the younger samples from loci 7230 and 7477, ΔR of *Terebralia palustris* and *Marcia spp.* Overlap (see Figure 3). With respect to differing diet and habitat this is unexpected. Recent observations report the occurrence of *Terebralia palustris* in regions without mangrove forests (Feulner 2000). This suggests that *Terebralia palustris* can also adapt to other feeding strategies than mangrove leaves. In addition, the Arabian Gulf consists of carbonaceous sediment (Lindauer 2019) which might cause ΔR for *Terebralia palustris* to be shifted towards older ages as well. Hence our result could mark the start of the local decline of mangrove forests possibly due to increased salinity and lack of freshwater input from rainfall. This is supported by the excavators' observation that *Marcia spp*. dominates the shell assemblages of the later contexts, a pattern also observed at Hamriya (~5 km south) possibly due to environmental causes (Händel 2009, 2014). To affirm this conclusion comparison to other environmental archives might help. During an earlier phase, represented in locus 6252, ΔR of these two species differ as expected with *Terebralia palustris* showing a lower ΔR than *Marcia spp*.

Throughout the data set, the internal scatter within the data for *Terebralia palustris* is larger than for the other species investigated. This might be due to a larger dependance of the respective shell regarding its position within the lagoon with respect to freshwater influx amount of limestone etc.

Mostly, *Hexaplex kuesterianus* points to a higher ΔR than Terebralia palustris but following similar pattern changes (see Figure 3B). Only at locus 7805 does ΔR overlap for both species with Hexaplex kuesterianus showing an even lower ΔR. This also suggests that Hexaplex kuesterianus does not

https://doi.org/10.1017/RDC.2025.19 Published online by Cambridge University Press

```
// Delta_R values updated for Marine20
Plot()
{
 Sequence()
 {
  Boundary("start 1");
  Phase("1")
  {
   Curve("Intcal20","Intcal20.14c");
   R_Date("19259 HK",3645,22);
   Curve("Marine20","Marine20.14c");
   Delta_R("19259_Hx",U(-300,300));
   R_Date("19261 Hx",4152,13);
  };
  Boundary("End 1");
  Boundary("start 2");
  Phase("2")
  {
   Curve("Intcal20","Intcal20.14c");
   R_Date("19421 HK",3440,23);
   Curve("Marine20","Marine20.14c");
   Delta_R("19421_Hx",U(-300,300));
   R_Date("19443 Hx",3881,18);
  };
  Boundary("End 2");
  Boundary("start 3");
  Phase("2")
  {
   Curve("Intcal20","Intcal20.14c");
   R_Date("19309 HK",3409,21);
   Curve("Marine20","Marine20.14c");
   Delta_R("19309_Hx",U(-500,500));
   R_Date("19311 Hx",4109,16);
  };
  Boundary("End 3");
  Boundary("start 4");
  Phase("3")
  {
   Curve("Intcal20","Intcal20.14c");
   R_Date("18618 HK",3063,23);
   Curve("Marine20","Marine20.14c");
   Delta_R("18618_Hx",U(-300,300));
   R_Date("18618 Hx1",3428,21);
   R_Date("18618 Hx2",3482,22);
   R_Date("18618 Hx3",3457,20);
  };
  Boundary("End 4");
 };
};
```

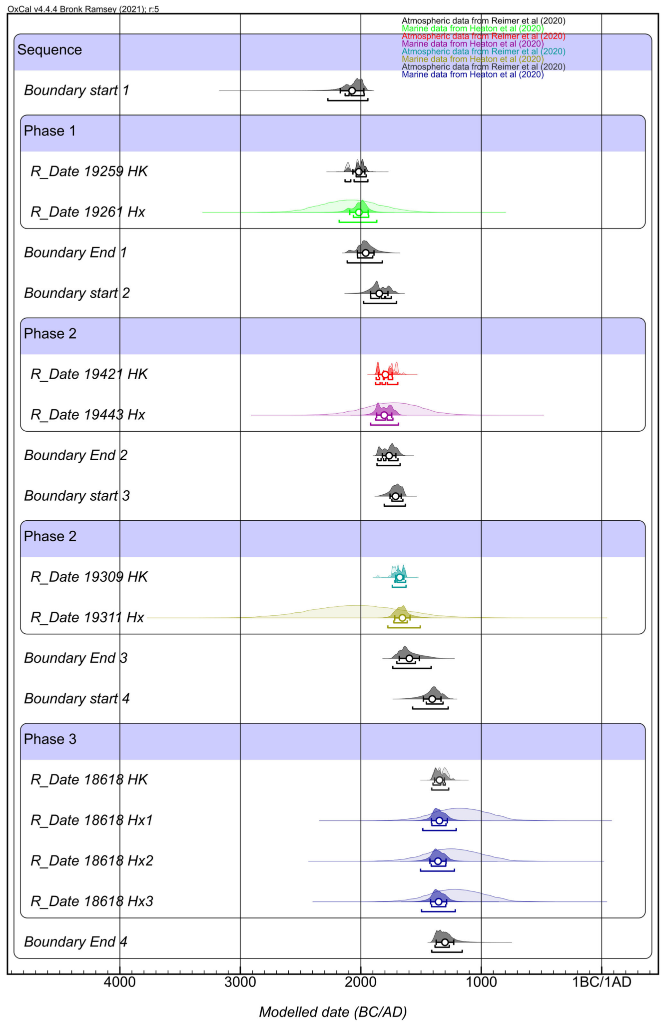

Figure 2. *Oxcal code (left) for modeling the reservoir effect of Hexaplex kuesterianus found in different layers at Tell Abraq and the resulting multiplot of the data. The reservoir effects of the other species were modeled accordingly (see supplement).*

primarily feed on *Terebralia palustris* when the data from locus 7805 can be explained by an increasingly divers influence on the ΔR of *T. palustris* as suggested above.

More charcoal fragments and shells per context can provide more reliable statistical models with the possibility to detect outliers. The loci with single pairs (7722, 7805 and 7720) might suffer from this and turn out to be challenging in their interpretation.

The results of this study confirm previous measurements on charcoal and charred date seeds (Magee et al. 2017, Table 1). They support chronological attribution of the artifactual material and field observations on stratigraphic relations (Table 2). Mixing or redeposition of single shells or charcoal fragment cannot be ruled out, even when trying to avoid sampling these layers as might be seen in locus 7484.

Correlation of the reservoir effect results to ΔR from other sites or other environmental information may provide explanations for the temporal variations (cf. Figures 3 and 4).

The gap to the older Umm al-Quwain–UAQ– (Méry et al. 2019) and Kalba ages is rather large and does not allow a conclusive interpretation. As the shells from Tell Abraq most probably originate from

https://doi.org/10.1017/RDC.2025.19 Published online by Cambridge University Press

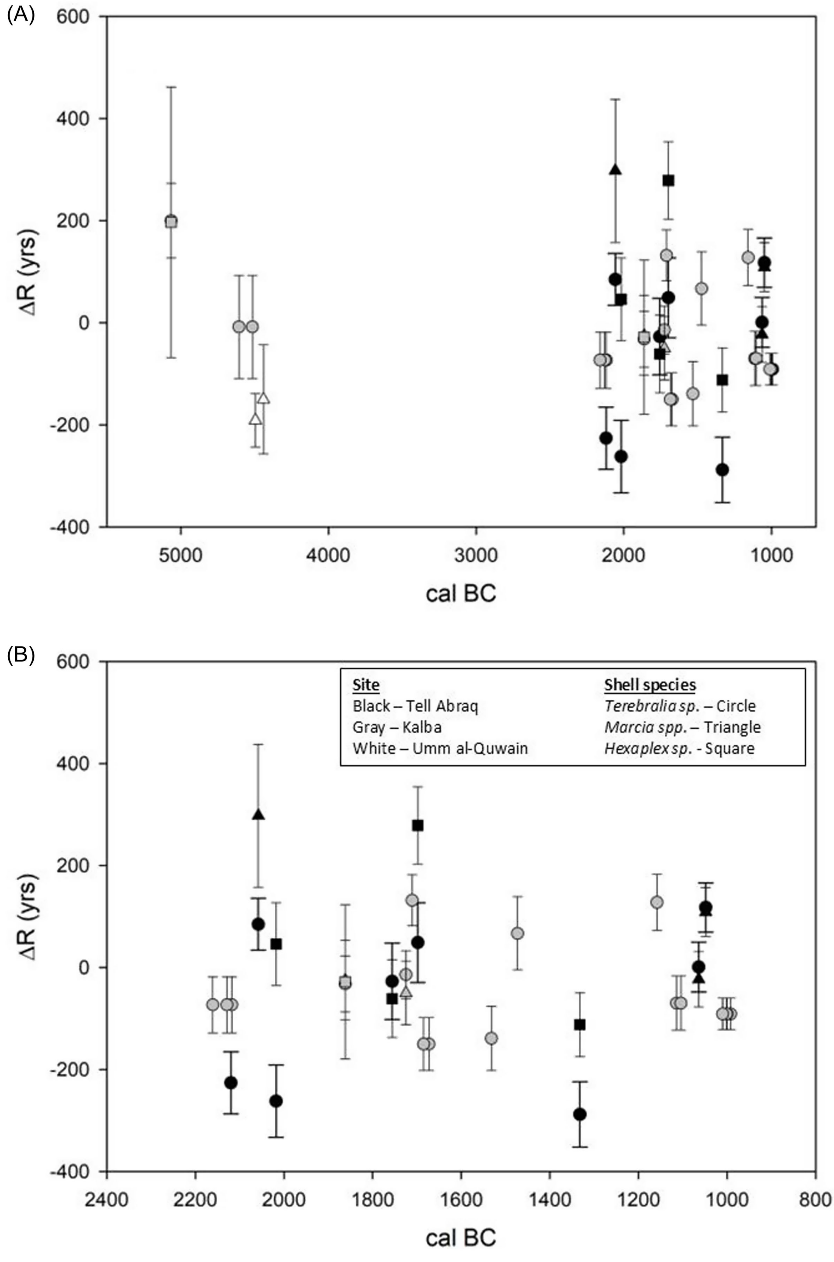

Figure 3. *(A) Results of shells from Tell Abraq compared to reservoir effects from other sites in the UAE, Umm al-Quwain northeast of Tell Abraq and Kalba at the Gulf of Oman. (B) Extract of younger period from (A). The samples from UAQ are published in Mery et al. (2019) and the data from Kalba in Lindauer et al. (2017) as well as Lindauer (2019).*

the Umm al-Quwain lagoon, changes in ΔR should be similar. Kalba on the Gulf of Oman first shows a decrease of ΔR over time before approaching a kind of wiggly plateau where it is difficult to derive a distinct trend (Figure 3A).

When comparing the results to sea-level data of the Arabian Gulf (Parker et al. 2018), there is no clear pattern in the phase younger than 2500 cal BCE (Figure 4). This is unexpected. The sea-level curve

https://doi.org/10.1017/RDC.2025.19 Published online by Cambridge University Press

https://doi.org/10.1017/RDC.2025.19 Published online by Cambridge University Press

Table 2. *Radiocarbon data with archaeological context. Chronology of the mentioned cultural phases follows Magee (Magee 2014): Umm an-Nar – 2700/2600-2000 BCE, Wadi Suq – 2000–1500 BCE, Late Bronze Age – 1500–1300 BCE, Iron Age I – 1300–1000 BCE, Iron Age II – 1000–600 BCE*

Labcode MAMS	Sample	**^{14}C yrs BP**	ΔR (mean, 2σ) yrs	Locus	Set	General setting	Stratigraphy	Cultural attribution (artifacts)
30528	*18243-1 date seed*	*2872 ± 20*		7230	67	Off-mound	Pre-Iron Age II	Late Bronze Age to Iron Age I
	Terebralia sp.		118± 48					
	Marcia sp.		109 ± 48					
30533	18597-2 charcoal	*2883 ± 21*		7477	73	Off-mound	Pre-Iron Age II	Iron Age I
	Terebralia sp.		1± 49					
	Marcia sp.		–23 ± 54					
32805	18618 charcoal	3063 ± 23		7493	73	Off-mound	Pre-Iron Age II	Late Bronze Age to Iron Age I
	Terebralia sp.		–288 ± 64					
	Hexaplex sp.		–112 ± 63					
46115	18605-1 charcoal	3074 ± 20		7484	73	Off-mound	Pre-Iron Age II	Early to Middle Bronze Age (red Barbar ware)
	Terebralia sp.		Not used					
35984	19309 charcoal	3409 ± 21		7722	None	On-mound (2nd terrace)	Post Umm an-Nar and pre-Late Bronze Age	Wadi Suq
	Terebralia sp.		49 ± 78					
	Hexaplex sp.		279 ± 76					
35983	19421 charcoal	3440 ± 23		7805	None	On-mound (2nd terrace)	Little earlier than 7722	Wadi Suq
	Terebralia sp.		–27 ± 75					
	Hexaplex sp.		–61 ± 76					
46121	19218 charcoal	3492 ± 21		7713	79	Off-mound	Pre-Iron Age II	Umm an-Nar to Wadi Suq
	Terebralia sp.		Not used					
35982	19259 charcoal	3645 ± 22		7720	79	Off-mound	Pre-Iron Age II	Umm an-Nar to Wadi Suq
	Terebralia sp.		–262 ± 71					
	Hexaplex sp.		46 ± 81					
35981	14593 charcoal	3668 ± 22		6252	15	On-mound (2nd terrace)	Pre-Middle Bronze Age fortification (pre-floor sequence; pre 7805+7722)	Umm an-Nar to Wadi Suq
	Terebralia sp.		85 ± 51					
	Marcia sp.		298 ± 140					
46123	19242 charcoal	3728 ± 26		7720	79	Off-mound	Pre-Iron Age II	Umm an-Nar to Wadi Suq
	Terebralia sp.		–2256± 61					

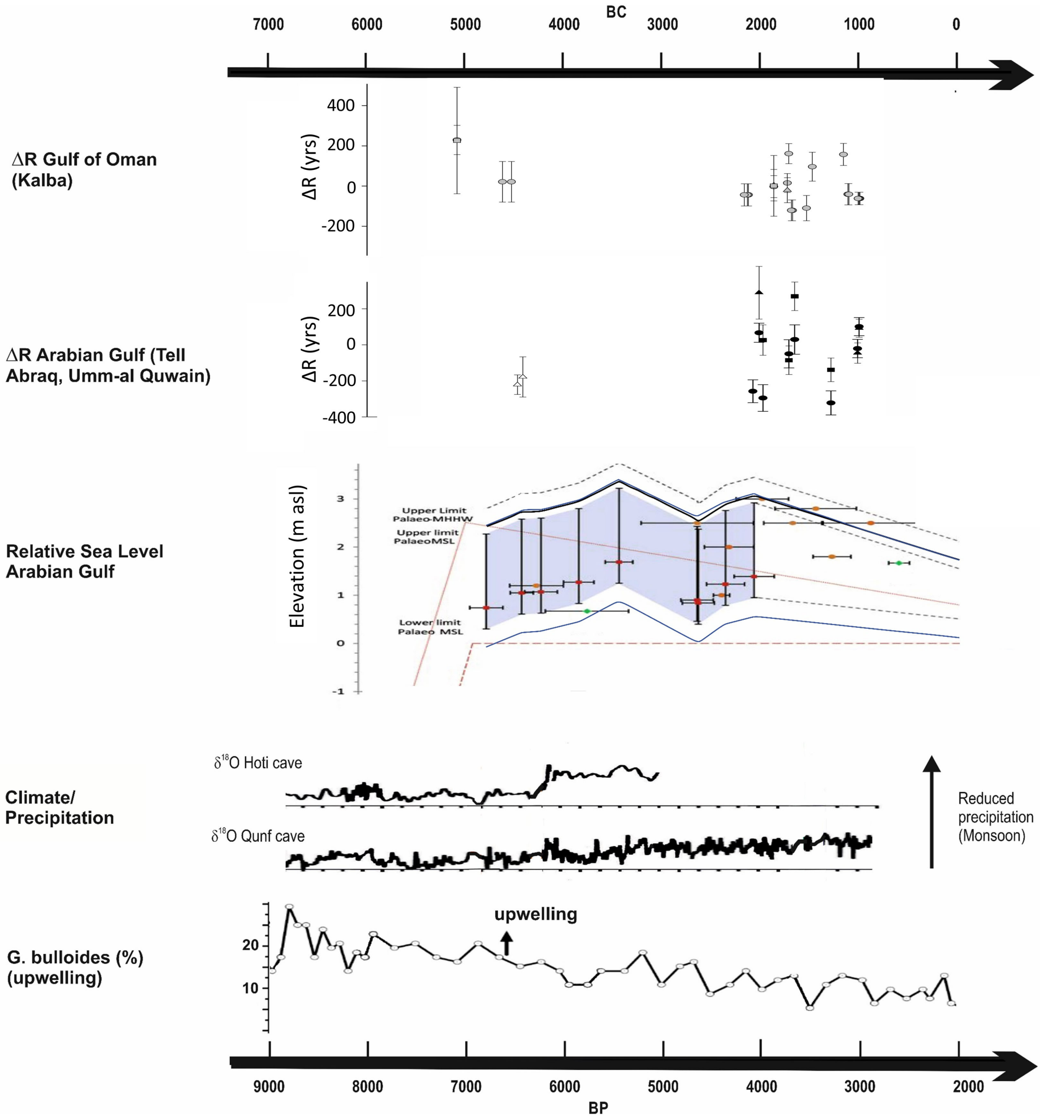

Figure 4. *Reservoir effects on shells from the UAE in the context of other paleoclimate data such as sea level in the Arabian Gulf (Parker et al. 2018): datapoints representing sea-level index points, rainfall taken from stalagmite records at Hoti and Qunf caves (both Oman; Fleitmann et al. 2007; Fleitmann and Matter 2009) and strength of upwelling along the coast of Oman indicated by foraminifera Globigerina bulloides (Gupta et al. 2003; Thamban et al. 2007). Note that the reservoir effect data on all shells from Tell Abraq, Umm al-Quwain and Kalba is presented separately to denote the differences between the two gulf areas.*

(Parker et al. 2018), shows a constant rise in the earlier phase and becomes increasingly variable towards younger ages, especially after 2500 cal BCE (Figure 4). The variation in ΔR during this period is larger than at Kalba which points to a larger variation between different locations within the lagoon maybe due to a reduced mixing as compared to Kalba. The shells at Tell Abraq hence reflect the combined influence of sea-level and lithology and location. The Tell Abraq data seems to swing around a plateau (Figure 3) which may be result of a combination of decreasing sea level, increasing salinity and high carbon content of the water smoothed slightly by exchange with atmospheric, hence fresh, ^{14}C.

https://doi.org/10.1017/RDC.2025.19 Published online by Cambridge University Press

Sediments around the Arabian Gulf are rich in carbonate (Lindauer 2019; Purser 1973). These carbonate-rich sands, evaporites and gypsum crystals (Omer 2010), can cause a rise in salinity when dissolved in the sea water and influence the radiocarbon signal depending on their respective ^{14}C content. On the other hand, the Arabian Gulf is rather shallow (maximum depth ~90 m). Even though this allows a thorough exchange with atmospheric ^{14}C, measurements in UAQ yielded slightly depleted ^{14}C water compared to Kalba (Lindauer 2019). The circulation is characterized by a surface inflow of water from the Gulf of Oman through the Strait of Hormuz. It exits the Gulf along the sea floor (Kämpf and Sadrinasab 2005) and travels south along the coast passing Khor Kalba. Khor Kalba is also influenced by the upwelling of old sea water from the Arabian Sea. Therefore, at Kalba, sea level, upwelling and outflow from the Arabian Gulf influence ΔR:

The data can further be compared to results from measurements on the foraminifera *Globigerina bulloides*, collected from sediment cores in the Arabian Sea (Gupta et al. 2003; Thamban et al. 2007). This species is an indicator for the strength of upwelling of cold and nutrient-rich (and ^{14}C-depleted) waters originating from the Southern Ocean. A reduced amount of *G. bulloides* is interpreted as reduced upwelling causing a reduction of ΔR in shells. Figure 4 shows a constant but oscillating decrease in *G. bulloides* throughout the Holocene. In Kalba, this is one reason for the drop in ΔR over time. For Tell Abraq, this might also be a reason for changes in ΔR, but with an oscillating ΔR; apparently other factors partly cancel this effect.

The occurrence of species is an indicator for changes in beneficial conditions for the respective species. *Anadara sp* can be found in Kalba since the early to mid-Holocene, in Umm al-Quwain during the mid-Holocene. At Tell Abraq, *Anadara spp.* is very rare. *Marcia s*pp. is found in Umm al-Quwain, but it is not very abundant before the Late Bronze Age and becomes dominant only in the Iron Age. In Kalba it does not occur before the Bronze Age.

A hint towards altered climatic conditions can be read from the speleothems. Stalagmites record rainfall in high resolution via the retained $\delta^{18}O$ composition. An increase in $\delta^{18}O$ is usually interpreted as a reduction in rainfall. Before 3000 BCE, stalagmites in Hoti cave (Central Oman) and Qunf cave (South Oman) recorded rising $\delta^{18}O$ values pointing to a reduction in rainfall over time with Hoti cave ceasing to grow around 3000 BCE (Fleitmann and Matter 2009; Fleitmann et al. 2007). This is interpreted as a shift of the Intertropical Convergence Zone (ITCZ) southward, leaving the Westerlies from the Mediterranean as the main source for rain. The amount of rain available directly influences the amount of freshwater input to the lagoon. The more freshwater is available, the more it can contribute to the reservoir effect of the shells depending on the ^{14}C content of the freshwater. A reduction leads to the ocean and underlying lithology as the dominant contribution to ΔR.

Conclusion

This study presents new radiocarbon data from the archaeological site Tell Abraq, UAE. Reservoir effects on species *Terebralia palustris, Marcia spp*., and *Hexaplex kuesterianus*, were determined for several settlement contexts at Tell Abraq ranging from Bronze Age to Iron Age. Apart from a detailed chronology of the site, the shell data points to changes in environmental conditions. No clear correlation of ΔR to the sea level curve for the Arabian Gulf could be shown. The data shows a rather wiggly appearance of ΔR towards younger ages. To provide a more profound interpretation requires more samples with larger datasets per phase that are definitely not mixed from same layers plus from other locations along the coast.

Supplementary material. To view supplementary material for this article, please visit https://doi.org/10.1017/RDC.2025.19

Acknowledgments. We would like to thank Sabah A. Jasim and Eisa Yousif from the Directorate of Antiquities, Sharjah, UAE, for their constant support and interest in our research. We are grateful to Axel Steinhof from MPI Biogeochemistry for supporting our study with measurements of samples. We thank the anonymous reviewers for their ideas and effort to help improve the manuscript.

Competing interests. The authors declare no competing interests.

References

Bernier P, Dalongeville R, Dupuis B and de Medwecki V (1995) Holocene shoreline variations in the Persian Gulf: Example of the Umm al-Qowayn Lagoon (UAE). *Quaternary International* **29–30**, 95–103.

Blau S (1996) Attempting to identify activities in the past: Preliminary investigations of the third millennium BC population at Tell Abraq. *Arabian Archaeology & Epigraphy* **7**, 143–176.

Culleton BJ, Kennett DJ, Ingram BL, Erlandson JM and Southon JR (2006) Intrashell radiocarbon variability in marine mollusks. *Radiocarbon* **48**(3), 387–400. doi: 10.1017/S0033822200038820.

Dalongeville R and Sanlaville P (2005) L'évolution des espaces littoraux du Golfe Persique et du Golfe d'Oman depuis la phase finale de la transgression post-glaciaire. *Paléorient* **31**(1), 9–26.

Degli Eposti M, Borgi F, Pellegrino M, Spano S, Abric C and Kannouma RH (2022) Renewed excavations at Tell Abraq, Umm al-Quwain, 2019–2020—Insights into the site's occupation from the mid-second millennium BC to the late pre-Islamic period. *Proceedings of the Seminar for Arabian Studies* **51**, 141–156.

Feulner GR (2000) The large mangrove mud creeper Terebralia palustris (Linneaus, 1767) in non-mangrove environments in Southeast Arabia. *Tribulus* **10**(2), 15–26.

Fleitmann D, Burns SJ, Mangini A, Mudelsee M, Kramers J, Villa I, Neff U, Al-Subbary AA, Buettner A, Hippler D et al. (2007) Holocene ITCZ and Indian monsoon dynamics recorded in stalagmites from Oman and Yemen (Socotra). *Quaternary Science Reviews* **26**(1–2), 170–188.

Fleitmann D and Matter A (2009) The speleothem record of climate variability in southern Arabia. *Comptes Rendus Geoscience* **341**(8–9), 633–642.

Gregoricka LA (2014) Assessing life history from commingled assemblages: The biogeochemistry of inter-tooth variability in Bronze Age Arabia. *Journal of Archaeological Science* **47**, 10–21.

Gupta AK, Anderson DM and Overpeck JT (2003) Abrupt changes in the Asian southwest monsoon during the Holocene and their links to the North Atlantic Ocean. *Nature* **421**, 354.

Hadden CS and Cherkinsky A (2016) Spatiotemporal variability in ΔR in the northern Gulf of Mexico, USA. *Radiocarbon*, 1–11. doi: 10.1017/RDC.2016.65.

Händel M (2009) Al-Hamriya (Sharjah, UAE)—Approaching an extensive shell midden site. In R MS de Beauclair and H Napierala (eds), *Knochen Pflastern Ihren Weg: Festschrift für Margarethe und Hans-Peter Uerpmann (German Title, Commemorative Volume)*, 103–112.

Händel M (2014) Al-Hamriya—Dynamik einer Muschelhaufenlandschaft in den Vereinigten Arabischen Emiraten. *Archaeologia Austriaca* **97–98**, 77–96 (in German).

Heaton TJ, Köhler P, Butzin M, Bard E, Reimer RW, Austin WEN, Bronk Ramsey C, Grootes PM, Hughen KA, Kromer B et al. (2020) Marine20—the marine radiocarbon age calibration curve (0–55,000 cal BP). *Radiocarbon* **62**(4), 779–820. doi: 10.1017/RDC.2020.68.

Kämpf J and Sadrinasab M (2005) The circulation of the Persian Gulf: A numerical study. *Ocean Science Discussions* **2**(3), 129–164.

Kromer B, Lindauer S, Synal HA and Wacker L (2013) MAMS—A new AMS facility at the Curt-Engelhorn-Centre for Archaeometry, Mannheim, Germany. *Nuclear Instruments and Methods in Physics Research Section B: Beam Interactions with Materials and Atoms* **294**(0), 11–13.

Lambeck K (1996) Shoreline reconstructions for the Persian Gulf since the last glacial maximum. *Earth and Planetary Science Letters* **142**(1–2), 43–57.

Lindauer S (2019) Radiocarbon Reservoir Effects on Shells from SE Arabia in the Context of Paleoenvironmental Studies. Doctoral thesis, Technical University Darmstadt.

Lindauer S, Hadden CS, Macario K and Guilderson TP (2022) Marine biogenic carbonates and radiocarbon—a retrospective on shells and corals with an outlook on challenges and opportunities. *Radiocarbon* **64**(4), 689–704. doi: 10.1017/RDC.2021.93.

Lindauer S, Marali S, Schöne BR, Uerpmann HP, Kromer B and Hinderer M (2016) Investigating the local reservoir age and stable isotopes of shells from Southeast Arabia. *Radiocarbon* **59**(2), 355–372. doi: 10.1017/RDC.2016.80.

Lindauer S, Santos GM, Steinhof A, Yousif E, Phillips C, Jasim SA, Uerpmann HP and Hinderer M (2017) The local marine reservoir effect at Kalba (UAE) between the Neolithic and Bronze Age: An indicator of sea level and climate changes. *Quaternary Geochronology* **42**(Supplement C), 105–116.

Magee P (2014) *The Archaeology of Prehistoric Arabia: Adaptation and Social Formation from the Neolithic to the Iron Age*. Cambridge: Cambridge University Press.

Magee P, Händel M, Karacic S, Brunet OFB, Uerpmann M, Uerpmann HP, Jameson M and Silvia Z (2018) Report on fieldwork at Muweilah and Tell Abraq, Emirate of Sharjah, United Arab Emirates 2014–2017. *Annual Sharjah Archaeology* **16** (second edition), 46–65.

Magee P, Händel M, Karacic S, Uerpmann M and Uerpmann HP (2017) Tell Abraq during the second and first millennia BC: Site layout, spatial organisation and economy. *Arabian Archaeology & Epigraphy* **28**, 209–237.

Magee P, Uerpmann HP, Uerpmann M, Jasim SA, Händel M, Barber D, Fritz C and Hammer E (2009) Multi-disciplinary research on the past human ecology of the east Arabian coast: Excavations at Hamriya and Tell Abraq (Emirate of Sharjah, United Arab Emirates). *Arabian Archaeology & Epigraphy* **20**, 18–29.

Méry S, Degli Eposti M, Aoustin D, Borgi F, Gallou C, Leroyer C, Lidour K, Lindauer S, Preston GW and Parker AG (2019) Neolithic settlement pattern and environment evolution along the coast of the northern UAE: The case of Umm al-Quwain UAQ36 vs. UAQ2 and Akab shell-middens. *Proceedings of the Seminar for Arabian Studies* **49**, 223–240.

Omer WMM (2010) *Ocean acidification in the Arabian Sea and the Red Sea*. University of Bergen.

Osterholz AJ, Baustian KM, Martin DL and Potts DT (2014) Commingled human skeletal assemblages: Integrative techniques in determination of the MNI/MNE. In AJO (ed), *Commingled and Disarticulated Human Remains*. New York: Springer, 35–50.

Parker A, Armitage S, Engel M, Morley M, Parton A, Preston G and Russ H (2018) Geomorphology, geoarcheology and paleoenvironments. *Dosariyah Reinvestigating a Neolithic Coastal Community in Eastern Arabia*. Archaeopress Publishing Ltd., 21–55.

Potts DT (1991) *Further Excavations at Tell Abraq: The 1990 Season*. Munksgaard.

Potts DT (1993) Four seasons of excavation at Tell Abraq (1989–1993). *Proceedings of the Seminar for Arabian Studies* **23**, 117–126.

Potts DT (2000) *Ancient Magan: The Secrets of Tell Abraq*. Trident Press.

Potts DT, Dalongeville R and Prieur A (1990) *A Prehistoric Mound in the Emirate of Umm al-Quwain, U.A.E.: Excavations at Tell Abraq in 1989*. Munksgaard.

Purser BH (1973) *The Persian Gulf: Holocene carbonate sedimentation and diagenesis in a shallow epicontinental sea*. Berlin: Springer-Verlag.

Ramsey CB (1995) Radiocarbon calibration and analysis of stratigraphy: The OxCal program. *Radiocarbon* **37**(2), 425–430. doi: 10.1017/S0033822200030903.

Reimer PJ, Austin WEN, Bard E, Bayliss A, Blackwell PG, Bronk Ramsey C, Butzin M, Cheng H, Edwards RL, Friedrich M et al. (2020) The IntCal20 Northern Hemisphere radiocarbon age calibration curve (0–55 cal kbp). *Radiocarbon* **62**(4), 725–757. doi: 10.1017/RDC.2020.41.

Tengberg M (2005) Les forêts de la mer. Exploitation et évolution des mangroves en Arabie orientale du Néolithique à l'époque islamique. *Paléorient* 39–45.

Thamban M, Kawahata H and Rao VP (2007) Indian summer monsoon variability during the Holocene as recorded in sediments of the Arabian Sea: Timing and implications. *Journal of Oceanography* **63**(6), 1009–1020.

Zazzo A, Munoz O, Badel E, Béguier I, Genchi F and Marcucci LG (2016) A revised radiocarbon chronology of the Aceramic shell midden of Ra's al-Hamra 6 (Muscat, Sultanate of Oman): Implication for occupational sequence, marine reservoir age, and human mobility. *Radiocarbon* **58**(2), 383–395. doi: 10.1017/RDC.2016.3.

Cite this article: Lindauer S, Händel M, and Magee P (2025). Reservoir Effects from Shells of Tell Abraq, Sharjah Emirate, UAE. *Radiocarbon* **67**, 600–612. https://doi.org/10.1017/RDC.2025.19